Proc. Natl. Acad. Sci. USA
Vol. 83, pp. 2899–2903, May 1986
Cell Biology

Three-dimensional structure of endosomes in BHK-21 cells

MARK MARSH*, GARETH GRIFFITHS†, GARY E. DEAN‡, IRA MELLMAN§¶, AND ARI HELENIUS§

*Chester Beatty Laboratories, The Institute of Cancer Research, Fulham Road, London SW3 6JB, United Kingdom; †European Molecular Biology Laboratory, Postfach 102209, 6900 Heidelberg, Federal Republic of Germany; and Departments of ‡Pharmacology and §Cell Biology, Yale University School of Medicine, 333 Cedar Street, New Haven, CT 06510

Communicated by George E. Palade, December 18, 1985

ABSTRACT **The organization of the endosome compartment in BHK-21 cells was studied by using horseradish peroxidase as a fluid-phase marker and Semliki Forest virus as an adsorptive marker. Stereo pairs of semithin sections (0.2–0.5 μm) and computer-aided reconstruction and tracing of serial thin sections (CARTOS) were used to obtain three-dimensional images of the labeled compartments. Two types of labeled organelles could be observed: (*i*) small vesicles and tubules (≈50 nm in diameter) and (*ii*) large complex structures consisting of central vesicular elements (with diameters up to 0.5 μm) and associated systems of radiating tubules. The large endosomes were located either in the peripheral cytoplasm or in the perinuclear region, and, importantly, they existed as independent organelles and not as an interconnected reticulum. Each endosomal vacuole had two to seven tubules oriented in random directions from the central vesicle. The tubules were 60–100 nm in diameter and up to 4 μm in length. Morphometric estimates indicated that 60–70% of the endosomal membrane was in the tubules, in contrast to 30–40% of the volume. No structural continuity between endosomes and Golgi cisternae was observed, although elements of the two systems were frequently found in close proximity.**

Endosomes constitute a ubiquitous prelysosomal compartment with critical functions in the endocytic pathway (1–3). They serve as intermediates in the transport of endocytosed ligands, fluid-phase components, and membrane components to lysosomes; they are involved in the dissociation of ligand–receptor complexes and the recycling of receptors and other plasma membrane components; and they constitute the major site for molecular sorting in the endocytic pathway (2–9). In some cell types, they also are thought to be involved in storage and processing of incoming ligands, regulation of receptor expression on the cell surface, and the maintenance of plasma membrane polarity (10, 11). Endosomes are, in addition, the sites of entry for certain enveloped viruses and bacterial toxins (12–15). Many of these functions depend on the acidic endosomal pH generated, at least in part, by proton-translocating ATPases (16–18).

Available data from thin-section and whole-mount preparations indicate that endosomes comprise an extensive system of vacuoles and membrane-bounded tubules (4–9, 19, 20). Here we have investigated the three-dimensional structure of endosomes and their overall organization in the cytoplasm by a combination of semithin-section electron microscopy and by computer-aided reconstruction of serial thin sections (CARTOS).

MATERIALS AND METHODS

Cells, Labeling, and Electron Microscopy. Baby hamster kidney (BHK-21) cells were maintained in minimal essential medium, Glasgow variation (G-MEM), with 5% fetal calf serum and 10% tryptose phosphate broth as described (12). For electron microscopy, monolayers of cells were grown to confluence (>48 hr) on 35-mm plastic tissue culture dishes.

Horseradish peroxidase (HRP; type II, Sigma) was used to label BHK-21 cell endosomes or lysosomes. For endosomes, the cells were incubated with HRP (10 mg·ml^{-1} in G-MEM) for either 15 min at 37°C or for 2 hr at 20°C (13, 17, 21). In some experiments, the endosomes were labeled with both Semliki Forest virus (SFV) and HRP; in this case, the cells were first incubated with 30 μg of SFV per ml in G-MEM at 0°C for 1 hr. The cells were then washed with 0°C medium and warmed to 37°C for 15 min in G-MEM containing HRP at 10 mg·ml^{-1} (13). To label the lysosomes, the cells were incubated with HRP for 15 min as above, washed, and then returned to culture for 2 hr in complete medium without HRP (13, 17). After the cells were labeled, they were washed rapidly with HRP-free medium and fixed for 30 min with cold 2.5% glutaraldehyde in 200 mM cacodylate buffer (12).

To visualize internalized HRP, fixed cells were washed with 200 mM sodium cacodylate (pH 7.2) containing 7.5% sucrose and were incubated with 0.1% diaminobenzidine dissolved in the same buffer. The reaction was initiated by adding H_2O_2 to 0.01% (1, 7). After 1 min in the dark, the diaminobenzidine solution was removed and the cells were washed, post-fixed with OsO_4, block-stained with uranyl acetate, dehydrated with ethanol, removed from the plastic with propylene oxide, and embedded as described (22). Semithin (0.25 μm) and thin sections (50 nm) were examined on a Phillips 400 electron microscope at 80 kV (thin) or 100 kV (semithin).

CARTOS. The CARTOS system for the reconstruction of serial sections has been described (23). Electron micrographs from serial sections were successively aligned in the *x* and *y* axes by correspondence with a suitably oriented starting frame. Image alignment was facilitated by using a video display monitor and storage system to alternately display the sample image and a stored image of the previous section. When aligned, the sample was photographed onto 35-mm film, and the video image of the sample was made the reference image for the next section. The aligned 35-mm movie served as the source for the reconstructions. Each frame was projected on a Vanguard film monitor equipped with a sonic digitizer; contours of interest were traced by hand with a digitizer probe, and the coordinates of these contours were entered into the files on a Codata microcomputer (CARTOS loaner system) or a PDP 11/34. Subsequently, these files were assembled by the CARTOS programs residing on a VAX 780 computer at Columbia University (New York, NY). An Evans and Sutherland picture system 2 was used to display the reconstructed images, and photographic images of selected orientations were taken directly from the screen.

The publication costs of this article were defrayed in part by page charge payment. This article must therefore be hereby marked "*advertisement*" in accordance with 18 U.S.C. §1734 solely to indicate this fact.

Abbreviations: HRP, horseradish peroxidase; SFV, Semliki Forest virus; CARTOS, computer-aided reconstruction of serial thin sections.

¶To whom correspondence should be addressed.

The CARTOS system is considerably more versatile than conventional modeling procedures. Reconstructions, such as the one illustrated in Figs. 5 and 6, can be completed in 3 hr, and the traces can be rapidly checked and edited. Furthermore, the picture system enables the entire reconstruction, or selected areas, to be examined by rotation about any chosen axis.

Stereology. Standard stereological techniques were used to quantify the relative distribution of membrane surface and internal volume associated with the vacuolar and tubular domains of the endosomes. HRP-positive endosomes in semithin sections or computer reconstructions (derived from thin sections) were analyzed by overlaying the images with a test grid consisting of 1-cm squares. The volume fraction was given by the frequency with which grid intersections fell within the vacuoles or tubules, and a surface area fraction was given by the frequency with which grid lines intersected with the limiting membrane of the vacuoles or tubules (24, 25). The tubular domains were defined as any HRP-labeled structure with an apparent diameter of <100 nm; all other labeled structures were classified as representing the vesicular domain. Since only relative surface and volume estimates were required, corrections for section thickness were not made (26).

RESULTS

Endosome Labeling with HRP and SFV. Endosomes do not have intrinsic properties that enable their unequivocal morphological identification. Consequently, endocytosed tracers such as viruses, colloidal gold conjugates, HRP-conjugates, and HRP have been used as functional markers (4–9, 19, 20). In our previous studies, we have used SFV, which is internalized by adsorptive endocytosis in BHK cells (10, 11, 27). However, the virus particles may not label all endosomes or be evenly distributed within individual endosomes. Therefore, in this study, we used a fluid-phase marker, HRP, which should be freely diffusible within endosomes and thus act as a marker for the entire compartment. Our previous studies on virus entry and endosome acidification have shown biochemically, by cell fractionation and by morphology, that BHK-21 cell endosomes are labeled with fluid-phase markers when cells are incubated for 15 min at 37°C or for 2 hr at 20°C (13, 17). In these cells, both fluid-phase and receptor-mediated endocytosis occur predominantly through coated pits and coated vesicles (28).

To confirm that HRP and SFV enter the same endosomes, cells were allowed to internalize both markers either at 20°C (2 hr) or for 15 min at 37°C. After fixation, the cells were treated with diaminobenzidine, embedded, and processed for thin-section electron microscopy. The electron dense HRP/diaminobenzidine staining was found in large (200–500 nm) profiles of irregular outline, shown later to represent vacuoles, and in small (50–100 nm) circular or elongated profiles, frequently located close to the large vacuoles and probably representing either vesicles or tubules. As previously described (13), some of the vacuoles contain vesicular profiles and are referred to as multivesicular endosomes. The reaction product was found in all SFV-containing endosomes (Fig. 1) and in some compartments lacking SFV, indicating more extensive labeling of endosomes with HRP. The viruses were preferentially located in the larger profiles, whereas HRP stained both large and small structures.

Endosome Morphology in Semithin Sections. The endosome compartment viewed in thin sections appeared as a heterogeneous population of different-sized profiles. To gain a better understanding of the overall spatial organization of these structures, we observed labeled endosomes in sections thick enough to contain a large portion of an endosome. Such semithin sections were particularly informative when viewed as stereo pairs, since they immediately indicate the shape and connections of the bodies represented by the various profiles seen in thin sections. Fig. 2 is a stereo pair of HRP-labeled endosomes in a 0.25-μm section; the label is contained in complex vesicular structures, which can be located in both the peripheral and perinuclear regions of the cells. No morphological distinctions could be made between endosomes in these different locations. Rather than a set of independent structures, the endosomes appeared as large, elaborate organelles with a central vacuolar body (300–500 nm in diameter) and several randomly oriented tubular extensions (50–60 nm in diameter and up to 4 μm in length). Accordingly, most of the smaller circular and elongated profiles seen in the thin sections were, in fact, part of these tubular extensions and, thus, connected to the larger endosomal vacuoles. Fig. 3 illustrates a group of perinuclear endosomes adjacent to the nuclear membrane and to several profiles of stacked Golgi cisternae. Again the vesicular components and extensive tubular systems can clearly be seen.

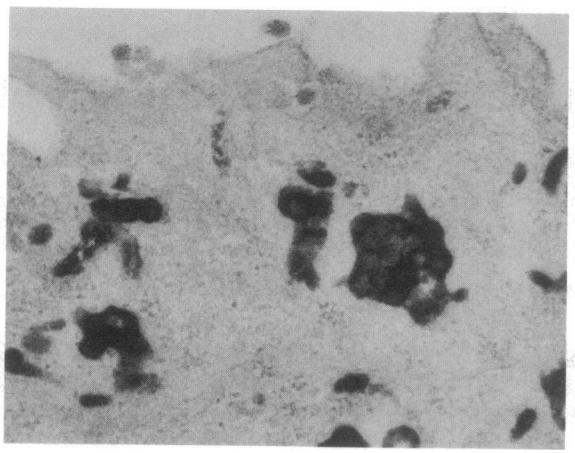

FIG. 1. Ligands internalized by fluid-phase endocytosis (HRP) and receptor-mediated endocytosis (SFV) enter the same endosomes. BHK cell monolayers on coverslips were incubated with 30 μg of SFV for 1 hr at 0°C in MEM. The cells were washed and warmed to 37°C in G-MEM containing HRP at 10 mg·ml^{-1} for 15 min. Subsequently, the cells were washed, fixed, and processed as described. Both SFV particles and HRP/diaminobenzidine reaction product are found within the same endosomal organelles. (×40,500.)

The semithin sections are useful for illustrating the three-dimensional organizations and complexity of the organelles. However, these sections can be misleading if the superimposition of images gives the impression of interconnection between structures (Fig. 2, uppermost two endosomes; Fig. 3, arrows). We could not distinguish between these two possibilities in stereo pairs of semithin sections or in thicker sections (0.5 μm) viewed by high-voltage electron microscopy. Hence, we have used computer-aided reconstruction of thin sections to obtain high three-dimensional resolution.

Reconstruction of Serial Thin Sections. Endosomes were reconstructed from serial thin (50 nm) sections by using CARTOS, an advanced graphics display program. One section from a consecutive series used for reconstruction is shown in Fig. 4. The contour coordinates of the HRP-containing vesicles were traced for each section, and the complete series was reconstructed and displayed on an Evans and Sutherland picture system 2. A group of three endosomes, obtained from one series of 18 sections, is shown in Fig. 5. The endosomes consist of a 200- to 500-nm vacuole portion from which extend a number of tubular processes, 50–60 nm in diameter. The central endosome is contained completely within the series and is not connected to structures outside these sections or to adjacent endosomes. The

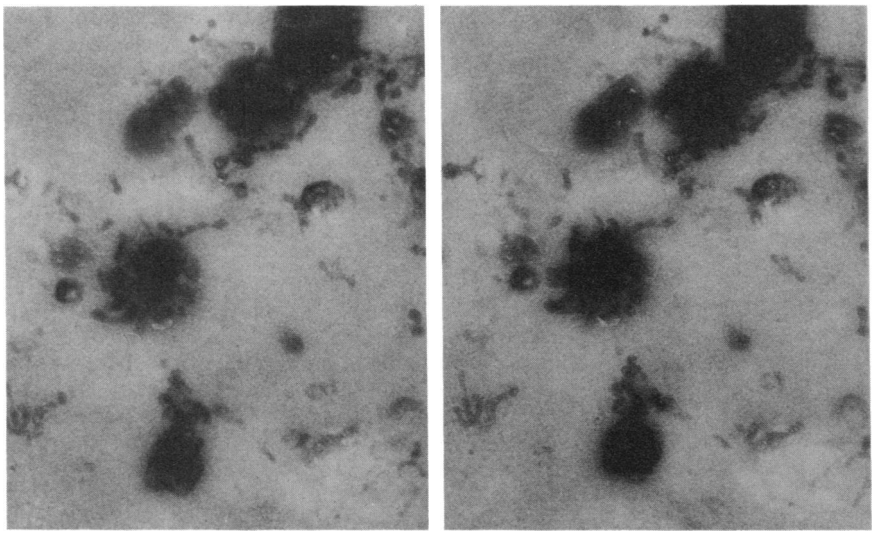

FIG. 2. Stereo-paired semithin-section electron micrographs of HRP-labeled endosomes. BHK-21 cells were incubated with HRP at 10 mg·ml^{-1} for 15 min at 37°C, fixed, and processed for electron microscopy. Semithin sections (0.25 μm) were cut and viewed without staining. The HRP/diaminobenzidine reaction product can be seen in an elaborate system of vacuoles and tubules. (×18,000.)

rotation facility of the Evans and Sutherland picture system enables the reconstructions to be viewed from different perspectives. In Fig. 6 the three endosomes in Fig. 5 have been rotated through 280°; the figure illustrates the point that, although the endosomes are independent structures, they may overlap and appear to be connected in some orientations (see Fig. 6*C*, arrow).

We have now reconstructed four series of sections containing a total of 16 complete endosomes; in one series, 8 complete endosomes were reconstructed. Each endosome had from two to seven associated tubules (approximate mean of six) with apparently random orientation. Upon analysis of the rotated images, we have not observed the tubules to connect individual endosomes. Although this analysis does not exclude the possibility that connections may exist transiently, it is clear that such connections are not frequent, even between closely apposed organelles. We conclude that the endosome compartment in BHK-21 cells, processed as described, is not an extensive reticulum but rather a set of individual organelles with complex morphology.

The thin-section reconstructions and the semithin sections have enabled us to examine both the organization and the spatial relationships between endosomes and other morphologically identifiable organelles. For example, perinuclear endosomes were often closely apposed to Golgi cisternae (e.g., Fig. 3). However, in reconstructions, we have not

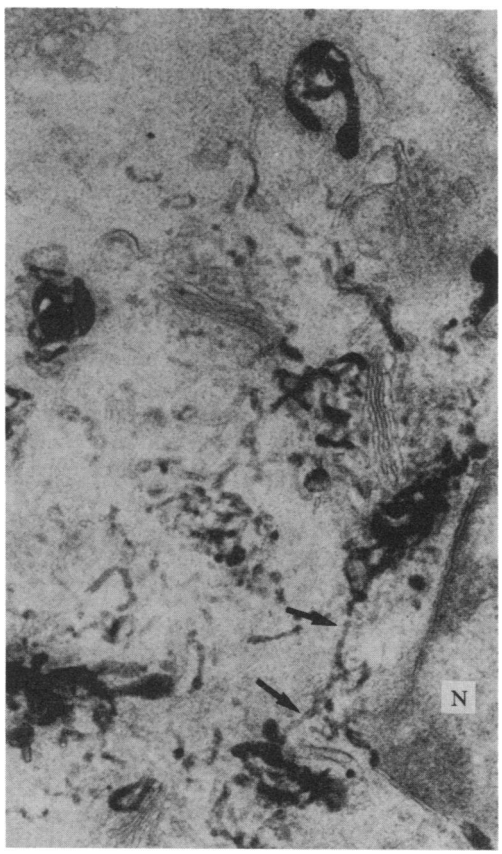

FIG. 3. Semithin-section electron micrograph of endosomes. BHK-21 cells were labeled as in Fig. 2. The endosome profiles in the perinuclear region of the cell are seen in close proximity to stacked cisternae of the Golgi complex. Arrows indicate tubular structures that may connect adjacent endosomes. N, nucleus. (×32,000.)

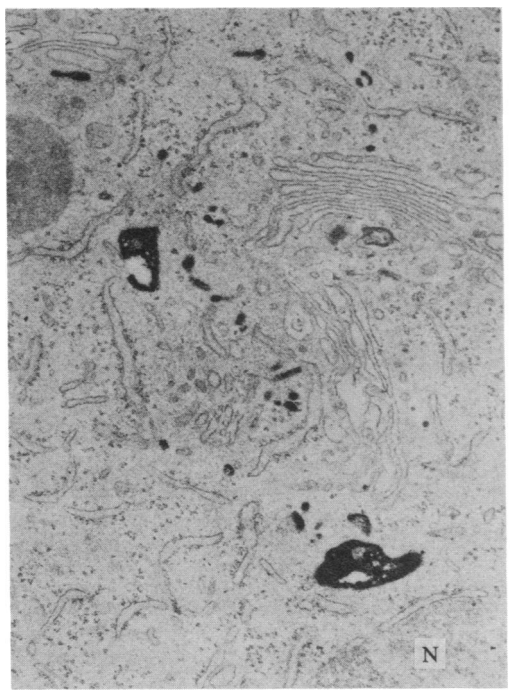

FIG. 4. Thin-section electron micrograph of endosomes. BHK cells were labeled and processed as described for Fig. 2, and 50-nm sections were cut. A representative section shown here displays a collection of HRP/diaminobenzidine-stained small vesicles in addition to several larger vacuolar structures. N, nucleus. (×29,600.)

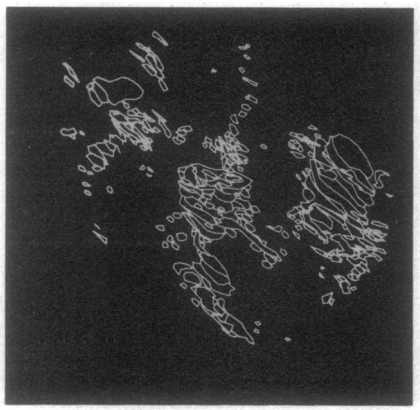

FIG. 5. CARTOS reconstruction of HRP-labeled endosomes. Eighteen serial sections (one of which is shown in Fig. 4) were used to reconstruct HRP-labeled endosomes by using the CARTOS system. The reconstructed image was displayed, with the hidden lines removed, on an Evans and Sutherland picture system and photographed directly from the screen. (×16,200.)

observed continuity of HRP-labeled endosomes with Golgi stacks.

Given the structure of the endosome, it seemed likely that most of its surface area was contained in the tubular extensions. This impression was confirmed by stereological analysis in both reconstructed images and semithin sections. From both measurements, we estimated that the tubules contained 60–70% of the total endosome surface area. In contrast, only 30–40% of the volume was located in the tubules, indicating that most of the endosome's fluid content (up to 70%) was contained in the vesicular portion. Since corrections for section thickness were not included, it is likely that the tubule volume was overestimated relative to the volume fraction contained within the vesicles (26). The determination of precise values must await a more detailed morphometric analysis.

In addition to the large vacuole/tubule system, we also observed in the reconstructions a number of profiles present in only one or two sections (see Fig. 5). These were usually short tubules or circular profiles of about 50-nm diameter. Thus, not all the HRP-positive small vesicular or tubular images seen in the thin sections were derived from sectioned extensions of larger endosomes but appeared to constitute separate structures.

Morphology of Lysosomes. In BHK-21 cells, internalized SFV and HRP are delivered to lysosomes after passing through the endosome compartment (13, 17, 28). We have established conditions to label the lysosome compartment with fluid-phase markers, and these organelles can be distinguished from endosomes by cell fractionation (17). In semithin sections (not shown), the lysosomes appear as nearly spherical bodies, often multivesicular, with very few of the tubular profiles that characterize the endosomes. The labeled organelles tended to be located in the perinuclear regions of the cells. On reconstruction, the lysosomes appear as a series of distinct, almost spherical, organelles (Fig. 7).

DISCUSSION

Previous studies using thin sections, whole-mount preparations, and frozen sections have shown that endosomes are organelles of considerable structural complexity (4–6, 8, 9, 13, 19, 20). The tubular extensions, the multivesicular vacuoles, and the dual distribution in the peripheral and perinuclear (centrosomal) regions are common features observed in many cell types (2). Here we describe the three-dimensional structure of BHK-21 cell endosomes identified by labeling with horseradish peroxidase. Our labeling criterion is based on a functional definition of endosomes as an early acidic endocytic compartment, which is the site of SFV penetration and which by cell fractionation can be biochemically distinguished from lysosomes and other organelles (2, 13, 17, unpublished data).

The results show that endosomes are morphologically complex organelles composed of a large vacuolar component and a number of associated tubules. The endosomes are not extensively interconnected and the tubules do not form an anastomosing reticulum. Furthermore, the studies indicate that most of the membrane surface area of endosomes residues in the tubular extensions, whereas the bulk of the endosome's volume is contained in the large vacuolar components. Given the complex structure and close proximity of endosomes to each other, this information could not have been derived by previously applied techniques. The studies illustrate the problems inherent in trying to determine the three-dimensional spatial organization of organelles from two-dimensional images and demonstrate the advantages of using a computer-based system to rapidly assemble and display reconstructed images in a form that can be viewed from all possible orientations.

The three-dimensional reconstruction showed the presence of small HRP-positive vesicles (about 40 in a region containing four endosomes) that were not connected to any larger membrane organelles. In view of the extensive membrane traffic and recycling occurring in the cell, the existence of such vesicles is not unexpected. Vesicles derived from the tubular extensions have been invoked to explain the selective

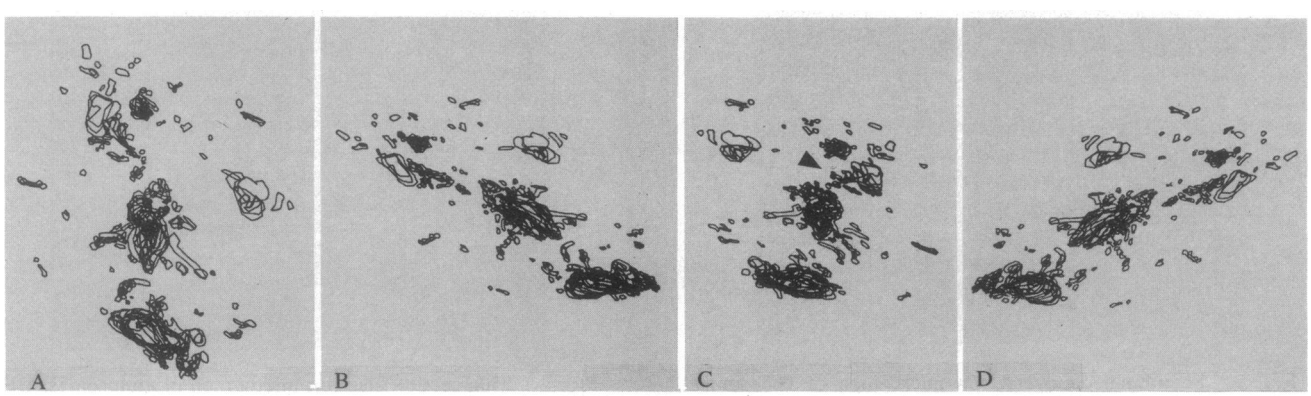

FIG. 6. Rotation series of reconstructed endosomes. The endosomes illustrated in Fig. 5 were rotated and displayed in different perspectives on the Evans and Sutherland picture system. This series was oriented around a vertical axis. Rotations were 0° (*A*), 95° (*B*), 208° (*C*), and 286° (*D*). The arrow indicates overlapping structures that appear to connect. (×12,100.)

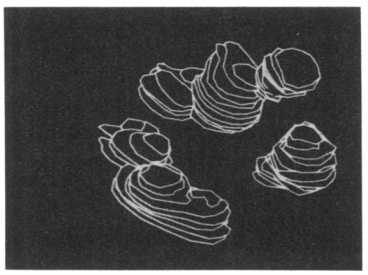

FIG. 7. CARTOS reconstruction of HRP-labeled lysosomes. BHK-21 cells were incubated with HRP at 10 mg·ml^{-1} for 15 min at 37°C, the HRP-containing medium was removed, and incubation was continued for 2 hr in HRP-free medium; the cells then were fixed and processed for electron microscopy, and the sections were reconstructed and displayed with the hidden lines removed. The lysosomes appear as free, nearly spherical structures. (×16,200.)

recycling of internalized membrane and receptors back to the plasma membrane (5, 8, 24). Moreover, HRP-positive vesicles are expected to occur as primary endocytic vesicles derived from the cell surface. The possibility that our results arise as a consequence of aldehyde-induced changes in morphology cannot be ruled out. However, the fact that extensive tubule systems are maintained after fixation and the fact that vesicles do not appear to be physically related to adjacent structures suggest that major alterations have not occurred. Previous studies, which by two-dimensional analysis have suggested extensive interconnections between endosomes, also relied on aldehyde fixation (4, 5).

That endosomes can constitute separate and independent organelles is important because it bears directly on their functions in the endocytic pathway. As separate membrane compartments, individual endosomes can display heterogeneity in composition, contents, and function. For example, the pH and ionic conditions may vary among individual endosomes; such variation would be reflected in differential effects on incoming ligand–receptor complexes, viruses, etc. It is already known that ligands internalized into endosomes may encounter decreasing pH conditions during their transit to lysosomes (18, 27, 29), a finding difficult to reconcile with a continuous, interconnected endosome compartment. Similarly with lysosomes, connections do not exist once lysosomal hydrolases are restricted to a subset of organelles. However, functional continuity must occur within the endocytic pathway to explain transit, and it can be assumed to be established by vesicular carriers, short-lived connections, or direct fusion.

Ligands internalized by receptor-mediated endocytosis are, as a rule, first routed into the peripheral endosomes and appear in the perinuclear endosomes some time later. Whether the transport occurs by carrier vesicles or by the movement of peripheral endosomes into the central cytoplasm remains an open question. Time-lapse photomicrographs of Cohn and co-workers (30–32) on macrophages and Herman and Albertini (33) on granulosa cells support the concept, however, that vectorial movement of endosomes from the periphery towards the nucleus can occur.

The reconstruction of complete large endosomal structures in three dimensions showed approximately six tubular extensions per endosome vacuole; in most cases, these appeared to be randomly oriented from the central body. The tubules accounted for about two-thirds of the surface area but only one-third of the volume. The estimate of surface to volume is consistent with the concept that the endosomal tubules mediate the recycling of membrane to the cell surface, while simultaneously allowing retention of most of the content (1, 34, 35).

We thank Professor Cyrus Levinthal, Tulla Lightfoot, Noel Kropf, and Steven Sterne of Columbia University for help with the CARTOS image reconstructions; Chris Hawes and members of the high-voltage electron microscopy unit at Oxford University; and Eva Bolzau and Anne Beidler for assistance with the electron microscopy. The helpful discussions with Professor George Palade are also gratefully acknowledged. This work was supported by National Institutes of Health Grants to I.M. (GM-29765, GM-33904), to A.H. (AI-18582), and to Cyrus Levinthal (P41RR00442). M.M. was a recipient of an award from the Swebilius Fund.

1. Steinman, R. M., Mellman, I. S., Muller, W. A. & Cohn, Z. A. (1983) *J. Cell Biol.* **96,** 1–27.
2. Helenius, A., Mellman, I., Wall, D. & Hubbard, A. (1983) *Trends Biochem. Sci. Endosomes* **8,** 245–250.
3. Brown, M. S., Anderson, R. G. W. & Goldstein, J. (1983) *Cell* **32,** 663–667.
4. Hopkins, C. R. (1983) *Cell* **35,** 321–330.
5. Geuze, H. J., Slot, J. W., Strous, G. J. A. M., Lodish, H. F. & Schwartz, A. L. (1983) *Cell* **32,** 277–287.
6. Willingham, M. C. & Pastan, I. (1980) *Cell* **21,** 67–77.
7. Straus, W. (1964) *J. Cell Biol.* **21,** 295–308.
8. Yamashiro, D. J., Tycko, B., Fluss, S. R. & Maxfield, F. R. (1984) *Cell* **37,** 789–800.
9. Abrahamson, D. R. & Rodewald, R. (1981) *J. Cell Biol.* **91,** 270–280.
10. Mellman, I., Plutner, H. & Ukkonen, P. (1984) *J. Cell Biol.* **98,** 1163–1169.
11. Pesonen, M. & Simons, K. (1984) *J. Cell Biol.* **99,** 796–802.
12. Helenius, A., Kartenbeck, J., Simons, K. & Fries, E. (1980) *J. Cell Biol.* **84,** 404–442.
13. Marsh, M., Bolzau, E. & Helenius, A. (1983) *Cell* **32,** 931–940.
14. Draper, R. & Simon, M. I. (1980) *J. Cell Biol.* **87,** 849–854.
15. Sandvig, K. & Olsnes, S. (1980) *J. Cell Biol.* **87,** 828–832.
16. Tycko, B. & Maxfield, F. (1982) *Cell* **28,** 643–651.
17. Galloway, C., Dean, G. E., Marsh, M., Rudnick, G. & Mellman, I. (1983) *Proc. Natl. Acad. Sci. USA* **80,** 3334–3338.
18. Merion, M., Schlesinger, P., Brooks, R. M., Moehring, J. M., Moehring, T. J. & Sly, W. S. (1983) *Proc. Natl. Acad. Sci. USA* **80,** 5315–5319.
19. Wall, D. A., Wilson, G. & Hubbard, A. L. (1980) *Cell* **21,** 79–93.
20. Gonatas, N. K., Stieber, A., Hickey, W. F., Herbert, S. H. & Gonatas, J. O. (1984) *J. Cell Biol.* **99,** 1379–1390.
21. Dunn, W., Hubbard, A. & Aronson, A. (1980) *J. Biol. Chem.* **255,** 5971–5978.
22. Griffiths, G., Warren, G., Quinn, P., Mathieu-Costello, O. & Hoppeler, H. (1984) *J. Cell Biol.* **98,** 2133–2141.
23. Macagno, E. R., Levinthal, C. & Sobel, I. (1979) *Annu. Rev. Biophys. Bioeng.* **8,** 323–351.
24. Steinman, R. M., Brodie, S. E. & Cohn, Z. A. (1976) *J. Cell Biol.* **68,** 665–687.
25. Weibel, E. R., Staubli, W., Gnagi, H. R. & Hess, F. A. (1969) *J. Cell Biol.* **42,** 68–91.
26. Weibel, E. R. & Paumgartner, D. (1978) *J. Cell Biol.* **78,** 584–597.
27. Tanasugaru, L., McNeil, P., Reynolds, G. T. & Taylor, D. L. (1984) *J. Cell Biol.* **98,** 717–724.
28. Marsh, M. & Helenius, A. (1980) *J. Mol. Biol.* **142,** 439–454.
29. Murphy, R. F., Powers, S. & Cantor, C. R. (1984) *J. Cell Biol.* **98,** 1757–1762.
30. Cohn, Z. A. & Benson, B. (1965) *J. Exp. Med.* **121,** 153–170.
31. Cohn, Z. A., Fedorko, M. E. & Hirsch, J. G. (1966) *J. Exp. Med.* **123,** 757–766.
32. Hirsch, J. G., Fedorko, M. E. & Cohn, Z. A. (1968) *J. Cell Biol.* **38,** 629–632.
33. Herman, B. & Albertini, D. F. (1984) *J. Cell Biol.* **98,** 565–576.
34. Van Deurs, B. & Nilausen, K. (1982) *J. Cell Biol.* **94,** 279–286.
35. Duncan, R. & Pratten, M. K. (1977) *J. Theor. Biol.* **66,** 727–735.